Fluorescent Photoaffinity Labeling of Cytochrome P450 3A4 by Lapachenole: Identification of Modification Sites by Mass Spectrometry†

Bo Wen,‡ Catalin E. Doneanu,‡ Carlos A. Gartner,§ Arthur G. Roberts,‡ William M. Atkins,‡ and Sidney D. Nelson*,‡

Department of Medicinal Chemistry, University of Washington, Box 357610, Seattle, Washington 98195, and Department of Cell Biology, Harvard Medical School, 240 Longwood Avenue, Boston, Massachusetts 02115

Received August 16, 2004; Revised Manuscript Received November 24, 2004

ABSTRACT: While photoaffinity ligands (PALs) have been widely used to probe the structures of many receptors and transporters, their effective use in the study of membrane-bound cytochrome P450s is less established. Here, lapachenole has been used as an effective photoaffinity ligand of human P450 3A4, and mass spectrometry data demonstrating the efficient and specific photoaffinity labeling of CYP3A4 by this naturally occurring benzochromene compound is presented. Without photolysis, lapachenole is a substrate of CYP3A4 and can be metabolized to hydroxylated products by this enzyme. A high-performance liquid chromatography/electrospray ionization mass spectrometry (HPLC/ESI-MS) procedure was developed to analyze small amounts of intact purified CYP3A4, and analysis of the labeled protein showed the presence of one molecule of lapachenole bound per monomer of protein. Photolabeled CYP3A4 peptide adducts were further characterized by mass spectrometric analysis after proteolytic digestion and isolation of fluorescent photolabeled peptides. Two peptide adducts accounting for >95% of the labeled peptides were isolated by HPLC, and both peptides, ECYSVFTNR (positions 97−105) and VLQNFSFKPCK (positions 459−469), were identified by nano-LC/ESI quadrupole time-of-flight (QTOF) and matrix-assisted laser desorption ionization time-of-flight (MALDI-TOF) mass spectrometry. The sites of modification were further localized to positions Cys-98 and Cys-468 for each peptide by nano-LC/ESI QTOF tandem mass spectrometry (MS/MS). The results provided the first direct evidence for interaction between the PAL and the putative B−B′ loop region, which may serve as a substrate access channel or as a part of the CYP3A4 active site. In conclusion, benzochromene analogues are effective PALs, which may be used in the study of other cytochrome P450 structures.

Cytochrome P450 (P450)[1] 3A4, the major P450 isoform present in human liver, is of particular clinical significance because of its ability to metabolize a large number of therapeutic agents of diverse structure (*1*). Moreover, intestinal CYP3A accounts for first-pass metabolism of therapeutic agents that alter CYP3A expression or activity, a significant potential for drug−drug interactions in vivo (*2*). Because of its general importance in drug metabolism and carcinogen bioactivation, elucidation of the key structural elements responsible for substrate recognition leading to oxidation by CYP3A4 is of considerable interest.

A number of techniques have been employed to locate active sites and substrate binding sites for enzyme−substrate complexes, including X-ray crystallography of the complex (*3*, *4*), spectroscopic analysis (*5*, *6*), site-directed mutagenesis (*7*−*9*), mechanism-based inhibition (*10*, *11*), and photoaffinity labeling (*12*, *13*). With eukaryotic cytochrome P450s, which are all intrinsic membrane proteins, the difficulty in obtaining an X-ray structure still has to be resolved, and most of our present knowledge has come from studies using site-directed mutagenesis and homology models based upon alignment of sequences with bacterial P450s (*14*−*16*) and modified forms of some mammalian P450s (*17*, *18*).

Photoaffinity labeling, like mechanism-based inhibition, has the advantage of providing direct information concerning the amino acid architecture of proteins in solution; however, photoaffinity ligands (PALs) do not require enzymatic activity to be utilized as active-site probes. While PALs have been widely used to probe the structures of many receptors and transporters, their effective use in the study of P450s remains limited. As reviewed by one of us (*19*), radiolabeled PALs have previously been used to probe cytochrome CYP1A and CYP2B structures. However, no PAL has been reported so far for CYP3A4, the major human liver P450

† This work was supported by NIH Grant GM32165 (to S.D.N.) and the UW NIEHS-sponsored Center for Ecogenetics and Environmental Health: NIEHS P30ES07033.

* To whom correspondence should be addressed: telephone (206) 543-1419; fax (206) 685-3252; e-mail sidnels@u.washington.edu.

‡ University of Washington.

§ Harvard Medical School.

[1] Abbreviations: CYP3A4, *Escherichia coli*-expressed poly(His)-tagged cytochrome P450 3A4; PAL, photoaffinity ligand; ESI-QTOF MS, electrospray ionization quadrupole time-of-flight mass spectrometry; MALDI-TOF MS, matrix-assisted laser desorption ionization time-of-flight mass spectrometry; CID, collision-induced dissociation; MS/MS, tandem mass spectrometry; DLPC, L-α-dilaurylphosphatidylcholine; DLPS, L-α-dilaurylphosphatidylserine; DOPC, L-α-dioleoylphosphatidylcholine; CHAPS, 3-(3-cholamidopropyl)dimethylammonio-1-propanesulfonate; GSH, glutathione (reduced); NADPH, nicotinamide adenine dinucleotide phosphate (reduced); CHCA, α-cyano-4-hydroxycinnamic acid; TFA, trifluoroacetic acid (CF_3CO_2H); FA, formic acid (HCO_2H).

10.1021/bi048228c CCC: $30.25
Published on Web 01/20/2005

Scheme 1: Formation of Michael Addition-type Lapachenole−Cysteine Adducts[a]

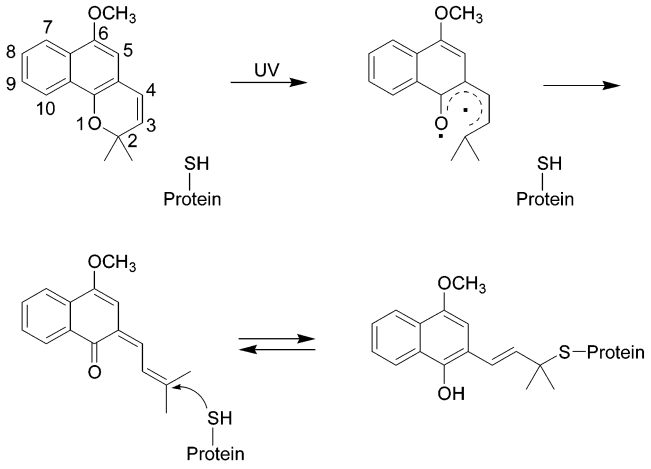

[a] Lapachenole is photoactivated by UV irradiation treatment and forms Michael addition-type adducts with cysteine residues from CYP3A4 protein.

isoform. Several studies (*20*−*24*) have shown that peptides from CYP1A and 2B family isoforms can be covalently modified with different types of radiolabeled PALs, which are usually native or chemically modified substrates. In these studies, photolabeled peptides have been partially characterized and have been predicted by molecular modeling to line substrate-binding regions of these enzymes. Nevertheless, in no study has the site of modification been absolutely characterized.

Lapachenole (Scheme 1) has been demonstrated to exhibit photochromic behavior to form a colored *o*-quinone allide after UV irradiation that converts back to the colorless benzochromene under ambient light (*25*). Previous work in our laboratory has shown that nucleophilic molecules, like glutathione, can trap this *o*-quinone allide intermediate to form lapachenole GSH conjugates (companion paper in this issue). NMR results suggested that the C-2 position of this *o*-quinone allide intermediate was bound to the sulfhydryl group of glutathione in the lapachenole−GSH conjugate. Evidence also was presented that lapachenole interacts with the active site of CYP3A4. CO binding spectra of CYP3A4 showed the conversion of the ferrous-CO P450 species to the inactive P420 form under photolytic conditions. Consistent with these results, substantial loss of enzyme activity toward two different substrates was observed when CYP3A4 was photolabeled by lapachenole. Finally, two different active-site-directed substrate/inhibitors of CYP3A4 blocked inactivation of CYP3A4 by lapachenole under photolytic conditions (companion paper in this issue).

In this study, we show that lapachenole is a substrate of CYP3A4 and provide the first mass spectrometric data demonstrating the efficient and specific photoaffinity labeling of CYP3A4 by this naturally occurring benzochromene compound. Application of an HPLC/ESI-MS technique made possible the detection of 1:1 adducts of lapachenole to CYP3A4, following photoaffinity labeling. Identification of the sites of covalent modification was achieved by isolating fluorescent photolabeled peptide fragments and identifying the adducted amino acid residues by CID mass spectrometry. Finally, in an attempt to gain a better understanding of the molecular basis for inactivation of CYP3A4 by lapachenole, we constructed complexed models for the identified adducts using the recent CYP3A4 crystal structures (*26*, *27*).

EXPERIMENTAL PROCEDURES

Materials. Lapachenole was synthesized in our laboratory as previously described (companion paper in this issue). DLPC, DOPC, and DLPS were purchased from Avanti Polar Lipids Inc. (Alabaster, AL). GSH, NADPH, imidazole, Triton X-100, CHCA, TFA, and anhydrous toluene were purchased from Sigma (St. Louis, MO). Sequencing-grade trypsin was purchased from Promega (Madison, WI). RapiGest SF was obtained from Waters (Milford, MA). Emulgen 911 was from Kao Chemicals (Tokyo, Japan). A Poros R2 perfusion column was from PerSeptive Biosystems (Cambridge, MA). HPLC solvents were of the highest grade commercially available and were used as received. All other reagents were analytical-grade.

Enzymes. Recombinant CYP3A4 was produced in *Escherichia coli* DH5α cells by use of the expression vector pCW 3A4-His6, kindly provided by Dr. Ron Estabrook. In a 2.8 L Fernbach flask, cells were shaken at 150 rpm and 27 °C for 48 h. Media and remaining expression conditions are as described by Gillam et al. (*28*). Pelleted cells were resuspended in resuspension buffer: 100 mM Tris-HCl (pH 7.4), 50 μM testosterone, and 20% glycerol with the addition of protease inhibitor cocktail from Sigma Chemical Co. (1 mL/L of initial culture volume). Lysozyme (5 mg/L) was added to the culture, which was allowed to stir at 4 °C for 1 h. Cells were homogenized and spun at 150000*g* and the yellowish supernatant was discarded. The pellet was resuspended in resuspension buffer by homogenization and allowed to stir at 4 °C for 1 h after the addition of 1% Emulgen 911. The solution was centrifuged at 150000*g*. The red/orange supernatant had imidazole added to a final concentration of 25 mM and was directly loaded onto ProBond nickel resin from Invitrogen. The column was washed with 20 column volumes of wash buffer: 100 mM Tris-HCl (pH 7.4), 20% glycerol, 40 mM imidazole, 0.05% cholate, and 50 μM testosterone. The column was eluted with a minimal volume of elution buffer: 100 mM Tris-HCl, pH 7.4, 20% glycerol, 500 mM imidazole, and 0.02% cholate. The eluted protein was dialyzed against 100 mM potassium phosphate, pH 7.4, in 20% glycerol and stored at −80 °C. Final yields after purification were typically 200 nmol/L of culture.

Both cytochrome b_5 and NADPH−cytochrome P450 oxidoreductase were expressed in *E. coli*. Human cytochrome b_5 expression plasmid was kindly provided by Dr. Ron Estabrook and expressed in BL21-DE3 cells under previously described conditions (*29*). Purification of cytochrome b_5 was similar to the purification of CYP3A4. Expression and purification of NADPH−cytochrome P450 oxidoreductase was accomplished as described by Chen et al. (*30*).

Instrumentation. Electrospray MS spectra of free and lapachenole-adducted CYP3A4 were recorded on a Quattro II triple quadrupole mass spectrometer (Micromass, Manchester, U.K.). Instrument settings were the following: source temperature 100 °C, nebulizing gas flow 20 L/h, N_2 drying gas 150 L/h, electrospray voltage 3.8 kV, and cone voltage 35 V. Data acquisition was carried out from *m*/*z* 500 to 2000 with a 5 s scanning time. Protein samples (∼300 pmol) were

injected on a Poros R2 perfusion chromatography column operated at a flow rate of 0.3 mL/min and interfaced on-line with the triple-quadrupole mass spectrometer. A Shimadzu LC10AD solvent delivery module (Shimadzu Scientific Instruments, Columbia, MD) was used to produce the following gradient elution profile: 10−50% solvent B in 5 min, followed by 50% B for 10 min and 50−90% B in 10 min (A = 5% acetonitrile, 0.05% TFA; B = 95% acetonitrile, 0.05% TFA).

MALDI-TOF MS analyses were performed on a Biflex III instrument (Bruker, Bremen, Germany). The MALDI probe was spotted with 1 μL of a 1:3 (v/v) mixture of the HPLC-purified sample containing the adducted peptides (0.5 μL) and a solution of CHCA prepared at 10 mg/mL in 50% acetonitrile/49.9% H_2O/0.1% TFA. The instrument was operated in the positive-ion mode with an accelerating potential of 20 kV and an extraction delay of 500 ns. A spectrum was produced by averaging data generated from 50 laser pulses.

On-line nano-LC/ESI MS/MS experiments were performed on an API-US QTOF mass spectrometer (Micromass, Manchester, U.K.) equipped with the CapLC system (Waters, Milford, MA). The stream select module was configured with an Opti-Pak Symmetry300 C_{18} trap column (Waters, Milford, MA) connected in series with a nanoscale analytical column. The latter was packed according to the pressurized bomb method described by Kennedy and Jorgenson (*31*) with a fused-silica column with an integral frit, PicoFrit (360 μm o.d. × 75 μm i.d. × 25 cm, 15 μm tip) obtained from New Objective (Cambridge, MA). In short, the end of the silica capillary that is to become the inlet was slipped through a seal into a pressure bomb containing a slurry of packing material (5 μm, 300 Å pore, Jupiter C_{18} silica gel particles from Phenomenex, Torrance, CA) dissolved in 2-propanol at a concentration of 25 mg/mL. The packing material was forced into the capillary by pressurizing the bomb to 1500 psi; about 2 h are required to pack a 20 cm long column. After the gas pressure was slowly released from the bomb, the inlet of the column was connected to an HPLC pump and flushed with acetonitrile for 2 h and Milli-Q water for another 2 h. The inlet end of the analytical column was connected to a ZU1XC metallic union (Valco, Houston, TX), where the electrospray voltage was applied.

HPLC-purified lapachenole peptide adducts (5 μL) were injected onto the trap column at 10 μL/min, cleaned up, and back-flushed to the analytical column at 0.5 μL/min by gradient elution. The gradient consisted of 5−50% solvent B for 30 min, followed by 50% B for 15 min and 50−90% B for 5 min (A = 5% acetonitrile, 0.1% FA; B = 95% acetonitrile, 0.1% FA); For metabolite studies, the HPLC gradient consisted of 5−70% solvent B for 40 min, followed by 70% B for 15 min and 70−90% B for 15 min (A = 5% acetonitrile, 0.1% FA; B = 95% acetonitrile, 0.1% FA).

QTOF parameters were set as follows: the electrospray potential was set to 3.5 kV (applied to the Valco union), the cone voltage was set to 40 V, the extraction cone was set to 2V, and the source temperature was set to 80 °C. In the case of peptide samples, the MS survey scan (*m*/*z* 400−1600) had a scan time of 1 s and the collision energy was set to 5 eV to minimize the decomposition of peptide adducts. For operation in the MS/MS mode, the scan time was increased to 2 s, the isolation width was set to include the full isotopic distribution of each peak (3 Da), and the collision energy was set to 25−35 eV. MS/MS spectra were recorded for the doubly charged molecular ions of adducted peptides; For metabolite studies, LC/MS runs were initially performed with 1 s survey scans (*m*/*z* 50−800) to fully characterize the chromatographic profile of all metabolites observed for *m*/*z* = 257.1. The corresponding MS/MS spectra were acquired in subsequent runs with a scan time of 2 s and a collision energy of 42 eV.

Lapachenole Metabolism by CYP3A4. Premixes of CYP3A4 were prepared as previously described (*32*) with minor modifications. The incubation mixture (500 μL) contained 0.3 μM CYP3A4, 0.6 μM NADPH−P450 reductase, 0.3 μM cytochrome b_5, and 0.2 mM lapachenole. The reaction was initiated by addition of 1 mM NADPH and quenched with 0.1 mL of ice-cold acetonitrile after 30 min of incubation at 37 °C. No NADPH was added in the control incubation. Samples (100 μL) were analyzed by LC/ESI MS as described above.

Photoaffinity Labeling of Cytochrome P450 3A4. The photochemical reactor consisted of a Mineralight Model UVGL-15 UV lamp (UVP Inc., San Gabriel, CA) and a sample holder mounted on a lab jack to allow sample height adjustment. The focus of the lamp was centered on the sample compartment at a lamp-to-sample distance of 1 cm. The enzyme solution to be photolyzed consisted of CYP3A4 (3 μM), DLPC (220 μg/mL), potassium Hepes (50 mM, pH 7.4), GSH (10 mM), and lapachenole (250 μM) in a final volume of 0.5 mL. The enzyme solution was first incubated at 37 °C for 15 min, and then the sample was photolyzed for 1 min taken at room temperature with filtered long-wavelength UV light (360 nm). The mixture was kept in the dark immediately after the irradiation and centrifuged at 14 000 rpm for 10 min. The supernatant was then analyzed by LC/ESI-MS as described above. The control sample was not photolyzed in the presence of the probe. For other samples, reductase and cytochrome b_5 were also added to test the labeling of coenzymes.

Proteolytic Digestion of CYP3A4. After photolabeling, samples were dialyzed against 50 mM ammonium biocarbonate at 4 °C by use of a Slide-A-Lyzer dialysis cassette (10 000 MWCO; Pierce, Rockford, IL). Modified CYP3A4 protein was then purified from other components by Poros R2 HPLC and evaporated to near dryness by a SpeedVac operated at room temperature. Samples were resuspended in 200 μL of 50 mM ammonium bicarbonate (pH 8.0) containing 0.2% RapiGest SF (Waters, Milford, MA). Upon addition of sequencing-grade trypsin (w/w 1:100), proteins were digested at 37 °C for 2 h. The reaction was quenched with 0.1% TFA.

Purification of Peptide Adducts by HPLC. Tryptic digests of CYP3A4 were separated by a Vydac C18 column (2.1 × 250 mm, Grace Vydac, Hesperia, CA). A Hewlett-Packard 1046A programmable fluorescence detector (Hewlett-Packard, Palo Alto, CA) was used in tandem with an Hewlett-Packard HPLC 1090 series II system (Hewlett-Packard, Waldbronn, Germany) to measure the amount of fluorescence, with excitation and emission wavelengths of 320 and 420 nm, respectively, and a bandwidth of 20 nm in each case. The flow rate was set at 0.3 mL/min. The gradient consisted of 12% solvent B for 5 min, followed by 12−90% B for 70 min (A = 5% acetonitrile, 0.05% TFA; B =

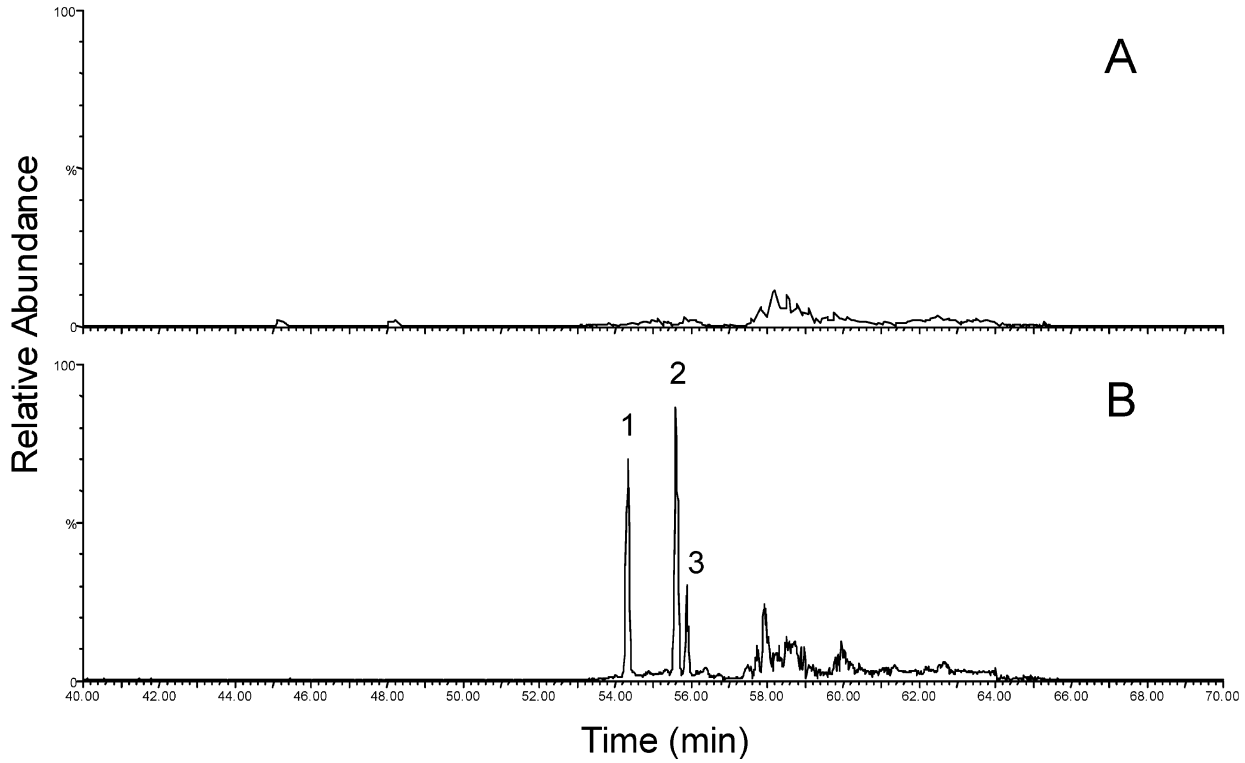

FIGURE 1: Reconstructed nano-LC/ESI MS ion chromatogram of *m*/*z* 257.1 for (A) control and (B) sample incubations of lapachenole with CYP3A4. The control incubation has no NADPH added. LC/MS runs were initially performed with 1 s survey scans (*m*/*z* 50−800) to fully characterize the chromatographic profile of all metabolites observed for *m*/*z* = 257.1.

95% acetonitrile, 0.05% TFA). Peaks that contained fluorescent peptide adducts were collected manually and subjected to mass spectrometric analysis.

Lapachenole Adducted CYP3A4 Crystal Structures. The lapachenole conjugate was drawn and the geometry was optimized by use of ArgusLab 4.0 (Planaria Software, Seattle, WA). This was aligned to Cys-98/Cys-468 of the recent crystal structure of engineered CYP3A4 (*26*; PDB code 1W0E) by use of DeepView 3.7 (*33*) and was then manually edited into the crystal structure. The structure was manipulated with WebLab Viewer Lite 4.0 (Accelrys, San Diego, CA) and ArgusLab 4.0, so that it was orientated in a geometrically reasonable position with no significant van der Waals overlap with the protein, providing us with a working model of photoprobe-bound CYP3A4.

RESULTS

Lapachenole Metabolism by CYP3A4. Lapachenole was a substrate for CYP3A4 and was metabolized in an NADPH-dependent reaction to three monooxygenated metabolites (Figure 1). LC/ESI MS/MS of the protonated molecular ions at *m*/*z* = 257.1 revealed two different kinds of oxidation products based on comparisons of the MS/MS spectra with that of lapachenole itself (Figure 2).

The more polar metabolite 1 (Figure 2B) showed major fragment ions at *m*/*z* = 229 ($MH^+ - 28$), *m*/*z* = 225 ($MH^+ - 32$), and *m*/*z* = 215 ($MH^+ - 42$). However, most informative is the lack of a fragment at *m*/*z* = 199, the base peak in the spectrum of lapachenole, which arises from loss of the elements of propylene from the C-2 dimethyl structure of the chromene ring. This means that oxidation did not occur in that structural unit. Although we have not fully characterized any of the metabolites, the significant ion at *m*/*z* = 229 for the loss the elements of CO suggests a carbonyl group that might have arisen from rearrangement of an initially formed epoxide at the 3,4-double bond of the chromene ring.

Metabolites 2 and 3 (Figure 2C) had essentially identical spectra indicative of isomeric oxygenation products. In contrast to metabolite 1, *m*/*z* = 199 was the base peak in their spectra, strongly indicative of oxidation of the C-2 methyl groups, which would give rise to geometric isomers. Fragment ions at *m*/*z* = 239 for the loss of H_2O, and at *m*/*z* = 227 for the loss of CH_2O, are consistent with C-2 hydroxymethyl metabolites. Again, this remains to be confirmed by NMR experiments. The main purpose of the results presented here is to show that lapachenole binds to the CYP3A4 active site as shown by the formation of oxidized products.

Purification of Covalently Modified CYP3A4. To decrease the complexity of the peptide pool generated from tryptic digestion of the incubation mixture, HPLC was used to separate b_5, P450 reductase, and CYP3A4. No major fluorescent signals were observed if the incubation mixture was not subjected to UV irradiation (Figure 3A). In contrast, two major fluorescent signals were observed at 9.5 and 22.0 min in the chromatogram after UV irradiation of the incubation mixture (Figure 3B). Mass spectrometric analysis of the intense peak eluting at 9.5 min revealed an $[M + H]^+$ ion at *m*/*z* 548.2, corresponding to the glutathione conjugate of lapachenole that has been previously characterized (companion paper in this issue). This is expected because of the high concentration of GSH present in the incubation mixture to reduce nonspecific protein labeling. The second fluorescent peak eluting at 22.0 min was presumably CYP3A4 apoprotein adducted with lapachenole (Figure 3B).

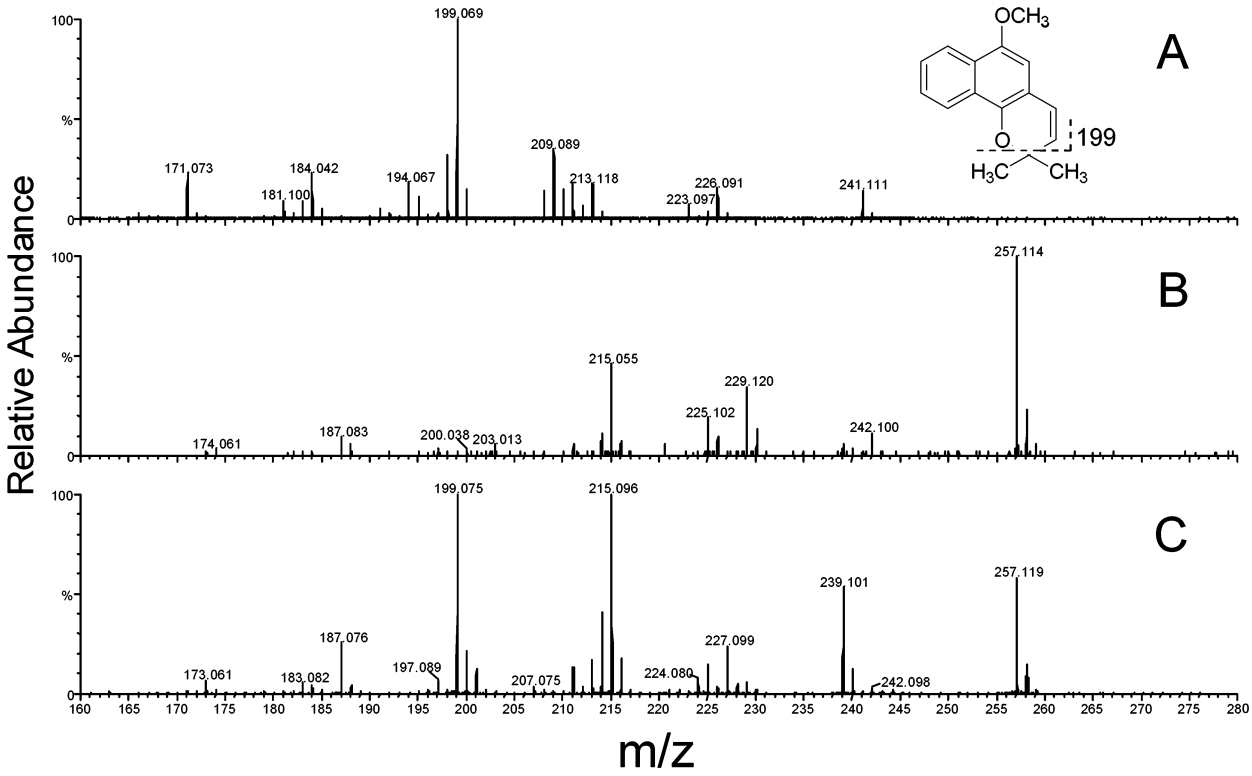

FIGURE 2: ESI MS/MS spectra of lapachenole and its CYP3A4 metabolites. Tandem mass spectra were obtained for the singly protonated ions at *m*/*z* 241.1 for lapachenole (A) and at *m*/*z* 257.1 for the monooxygenated metabolites 1 (B) and 2 (C) at a collision energy of 42 eV as described under Experimental Procedures.

Characterization of Lapachenole Adducts of CYP3A4. To further verify that lapachenole formed adducts with CYP3A4, the fluorescently tagged protein was subjected to HPLC/ESI-MS. Intact and modified CYP3A4 were separated from the other components of the reconstituted system by HPLC prior to mass spectrometric analysis as described under Experimental Procedures. For each protein, an experimentally determined molecular mass (MM) was calculated from the observed charge state distribution, or ion envelope (usually made up of 30−40 charge states), that possessed a sample-to-sample standard deviation of less than 0.05%. The predicted average MM of CYP3A4 based on protein sequence is 57 244 Da. As shown in Figure 4, the analysis of the native CYP3A4 revealed a peak at *m*/*z* 57 280 ± 3 (the inset). The difference between the average of the experimentally determined MM (±SD, based on experiments performed at least three different times) and the predicted average MM of CYP3A4 was 0.06%. When the enzyme was photolyzed with 0.25 mM lapachenole in 50 mM potassium Hepes buffer at room temperature, two protein species were detected with MMs corresponding to CYP3A4 apoprotein and monoadducts that incorporated one molecule of lapachenole into one CYP3A4 protein (Figure 4). The average MMs of apo-CYP3A4 and monoadduct of CYP3A4 were experimentally determined to be 57 280 ± 3 and 57 520 ± 3 Da, respectively. Both protein species were coeluted at 22.0 min during a 30 min gradient run on a Poros R2 column. On the basis of the peak heights, approximately 60% of the total native CYP3A4 protein was covalently labeled by lapachenole after 1 min of UV irradiation. The mass shift of 240 Da for the adducted CYP3A4 protein suggested that one molecule of lapachenole was bound specifically per CYP3A4 protein and the labeling was irreversible under these severely denaturing HPLC conditions. No other adducts were detected associated with the b_5, P450 reductase, or heme of CYP3A4 in the LC/ESI MS analysis (Supporting Information).

Purification of CYP3A4 Peptide Adducts. Covalently modified CYP3A4 protein was purified from the incubation mixture by HPLC on a Poros R2 column. To characterize the structural modification of CYP3A4 by lapachenole, the modified CYP3A4 (~500 pmol) was digested with sequencing-grade trypsin and analyzed by HPLC coupled with UV detection at 214 nm and fluorescence detection with 320 and 420 nm as excitation and emission wavelengths, respectively. More than 40 peptide peaks (Figure 5A) were detected by UV detection at 214 nm during a 90-min gradient run. However, as shown in Figure 5B, only two major fluorescent peptide peaks (P-1 and P-2) were observed. Fluorescence from these two peaks accounted for approximately 95% of the total fluorescence from tryptic digestion of the CYP3A4 adduct. The relative ratio between peak P-1 at 24.6 min and peak P-2 at 25.1 min was 1:0.75. Since the analysis of labeled intact CYP3A4 protein by HPLC/ESI-MS showed that one molecule of lapachenole bound per monomer of protein, peptide adducts P-1 and P-2 represented either distinct monomeric CYP3A4 adducts or a single adduct of a miscut peptide.

In a subsequent experiment, the fluorescent peptide peaks were collected manually for further analysis. To test the stability of these peptide adducts, the collected fluorescent fractions were reanalyzed by HPLC. Greater than 90% of the total amount of fluorescence associated with each peptide adduct was detectable in the second HPLC chromatographic run.

Identification of Lapachenole Modification Sites by MALDI-TOF MS and Nano-LC/ESI QTOF MS/MS Analysis. In the

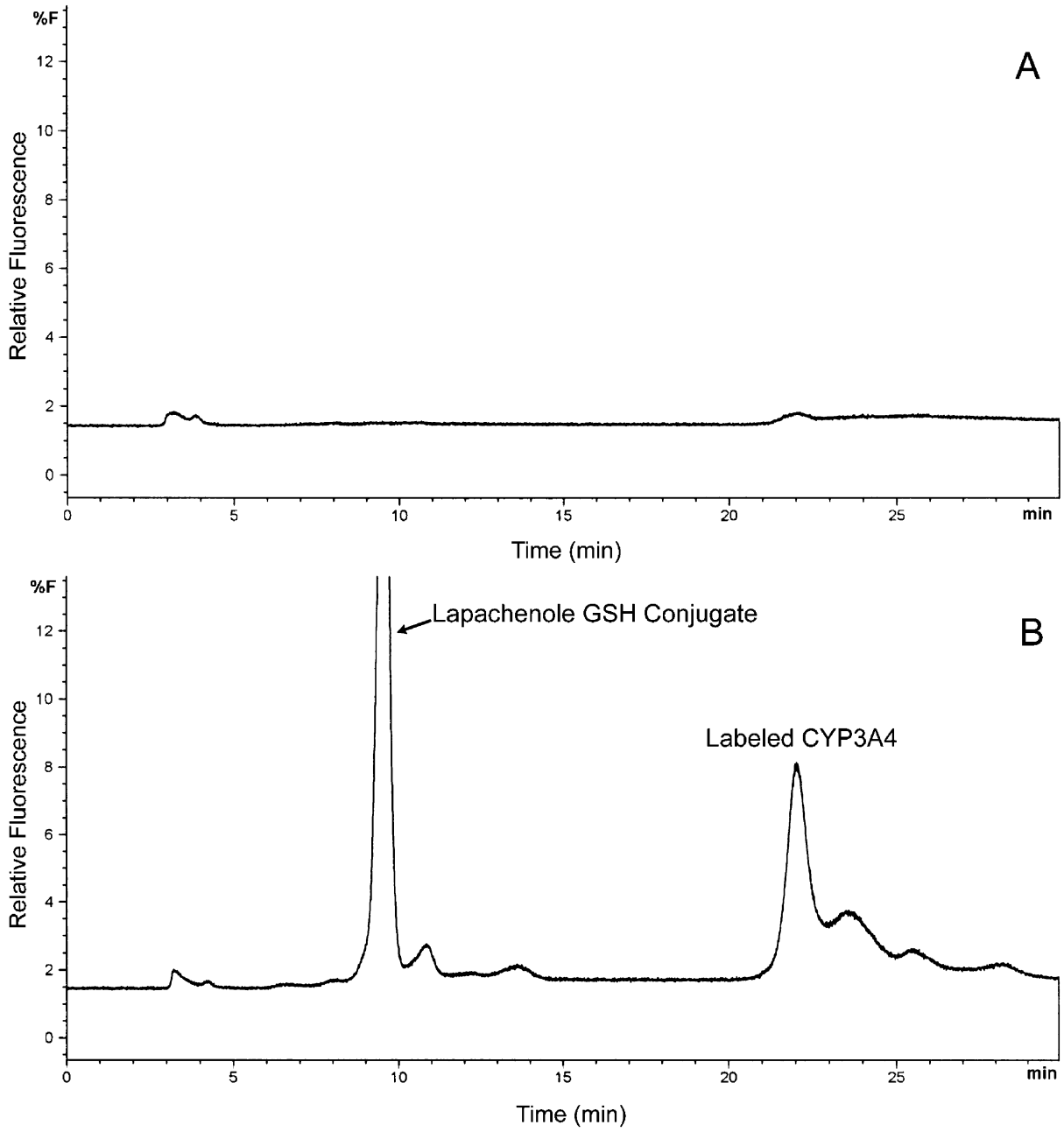

FIGURE 3: Covalent binding of photolyzed lapachenole to CYP3A4: HPLC separation of the components of the reconstituted CYP3A4 system after exposure to lapachenole plus photolysis as monitored by fluorescence detection. (A) Nonphotolyzed control; (B) photolyzed sample. Lapachenole GSH conjugate and P450 eluted at 9.5 and 22.0 min, respectively. Cytochrome b_5, P450 reductase, and heme elute at 12.5, 15.6, and 6.2 min, respectively. Fluorescence absorption occurring after 22 min was not associated with lapachenole or proteins but rather appeared to derive from lipids.

MALDI-TOF MS analysis, the peptide adduct P-2 was observed in both adducted form and free form at *m*/*z* 1550.8 and 1310.7, respectively (Figure 6). The loss of photolabel was presumably due to the high energy from the laser beam in the MALDI-TOF MS. This hypothesis is supported by the fact that only adducted peptides were observed for P-1 and P-2 during the primary ESI/MS analysis but not in CID analysis (see below). Because of this stability issue, only the free peptide form was observed for P-1 at *m*/*z* 1118.5 but not the adducted form (Figure 6). Interestingly, we also found two oxidized peptide adducts for P-1 and P-2 at *m*/*z* 1374.6 and 1566.8, respectively (Table 1). The exact mechanism for this oxidation remains unknown.

To identify sites on CYP3A4 adducted by lapachenole, the collected fluorescent HPLC fractions containing lapachenole-modified fragments were further analyzed by LC/ESI MS/MS. Adducted peptides P-1 and P-2 were eluted at 34.5 and 36.3 min, respectively, during the LC/MS analysis (Figure 7A). The MS/MS spectrum of the doubly charged $[M + 2H]^{2+}$ ion at *m*/*z* 679.80 from the lapachenole-modified peptide (P-1) with the sequence Glu-Cys-Tyr-Ser-Val-Phe-Thr-Asn-Arg is shown in Figure 7B. In the MS/MS analysis, the singly charged fragment ions (b_4-b_6 and y_1-y_8) and corresponding ions with loss of H_2O or NH_3 (b_{4-18}, b_{5-18}, y_{2-17}, y_{3-17}, and y_{4-17}) were observed. In this spectrum, the singly charged free peptide ion at *m*/*z* 1118.53 and ion resulting from dehydration at *m*/*z* 1100.52 were observed along with the lapachenole fragment ion at *m*/*z* 199.08, suggesting that some of the photolabel was lost during the collision-induced dissociation (CID) analysis. The mass of

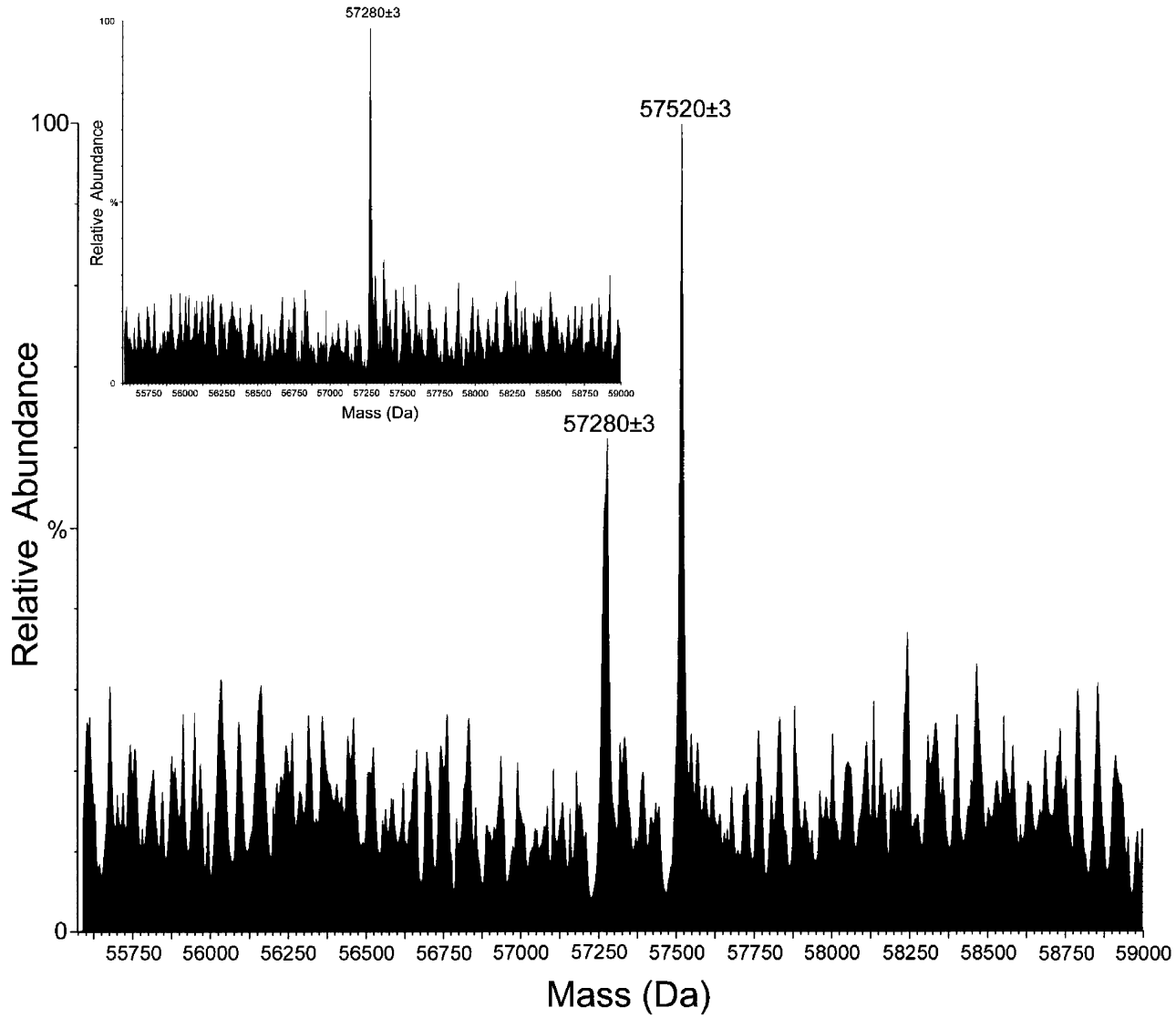

FIGURE 4: LC/ESI-MS analysis of CYP3A4 photolabeled with lapachenole. Samples were incubated with lapachenole with or without photolysis and analyzed as described under Experimental Procedures. Deconvoluted spectrum of the apo-CYP3A4 photolabeled with lapachenole (molecular mass = 57 280 ± 3 Da, $n = 6$) is shown. (Inset) Deconvoluted spectrum of apo-CYP3A4 from a control incubation (molecular mass = 57 520 ± 3 Da, $n = 6$).

the fragment ion b_5, *m*/*z* 822.42, was 240 Da greater than expected for the peptide fragment alone, suggesting that the lapachenole modification site is close to the N-terminus of the peptide. Moreover, the mass of the singly charged N-terminal product ion y_8 was also observed to increase 240 Da (*m*/*z* = 1229.61), and no other mass shifts were detected for the rest of y ions. These results showed that the lapachenole modification site was located at the N-terminus on Cys-98. The MS/MS spectrum of the doubly charged $[M + 2H]^{2+}$ ion at *m*/*z* 775.90 from the lapachenole-modified peptide (P-2) with the sequence Val-Leu-Gln-Asn-Phe-Ser-Phe-Lys-Pro-Cys-Lys is shown in Figure 7C. In the MS/MS analysis, the singly charged fragment ions (b_3-b_8 and y_3-y_{10}) were observed. In this spectrum, the singly charged free peptide ion at *m*/*z* 1310.74 and ion resulting from dehydration at *m*/*z* 1292.74 were observed together with the lapachenole $[M + H]^+$ ion at *m*/*z* 241.10, again indicating that some lapachenole was lost during the CID process. The reason that lapachenole was not fragmented to *m*/*z* 199.08 in this spectrum remains unknown. The doubly charged free peptide ion at *m*/*z* 655.87 was also observed. In the MS/MS analysis, the masses of the C-terminal fragment ions (y_3 and y_6) were observed to increase 240 Da, and no mass shifts were detected for the observed b ions (b_3-b_8). These data suggest that the lapachenole modification site was located on the C-terminus of the peptide, associated with Cys-468. Thus, the target amino acids of the lapachenole modification in CYP3A4 are apparently cysteine residues. Together with the ESI/MS results of photolabeled CYP3A4, these observations suggested that two cysteine residues (Cys-98 and Cys-468) were modified by lapachenole, but only one molecule of lapachenole bound per monomer of protein.

Lapachenole Adducted CYP3A4 Crystal Structures. On the basis of the complexed structure constructed from the PDB file 1W0E, Cys-98 is located within the putative B−C helix loop region. Figure 8A shows that the photolyzed lapachenole bound to the sulfhydryl group of Cys-98 is located in the putative B−B′ loop, a region of CYP3A4 that has previously been shown to have a profound effect on catalysis and substrate recognition (*34*). The CYP3A4 active-site heme group is within approximately 7 Å of the Cys-98 lapachenole adduct in this complexed structure. Figure 8B shows that

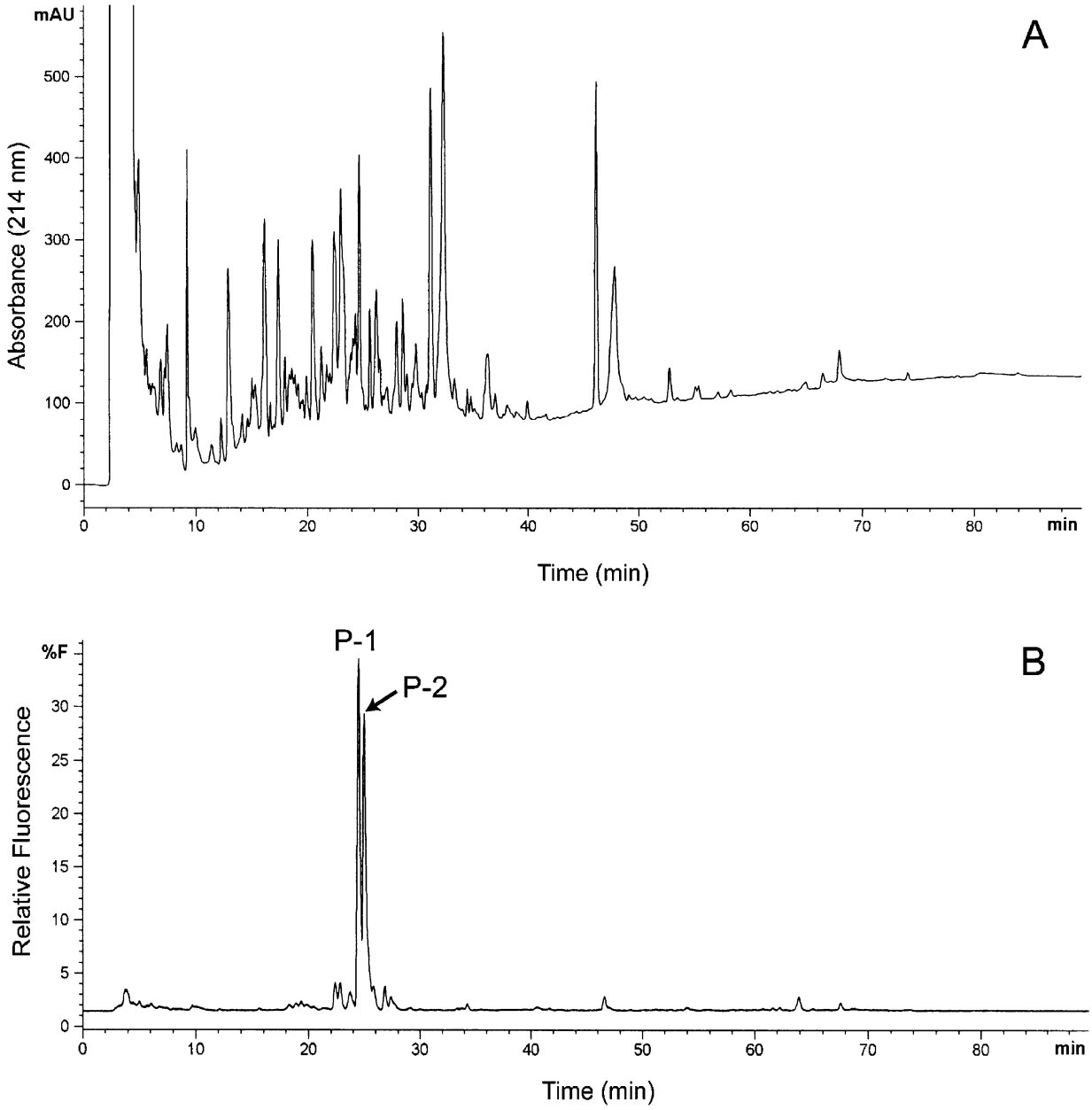

FIGURE 5: Fluorescence detection of CYP3A4 tryptic peptide adducts photolabeled with lapachenole. HPLC separation of the proteolytic digests of the lapachenole labeled CYP3A4 were monitored by (a) variable-wavelength detection at 214 nm and (b) fluorescence detection with 320 and 420 nm as excitation and emission wavelengths, respectively. The fraction containing the two major fluorescence peaks eluted at 24.6 and 25.1 min were collected and analyzed by nano-LC/ESI MS/MS.

the Cys-468 lapachenole adduct is positioned at the end of the L-helix on which the cysteinal heme ligand, Cys-442, is located.

DISCUSSION

Previously (companion paper in this issue) we found that several chromenes were photoactivated to structures that rapidly underwent Michael addition reactions with glutathione (GSH) and that one of these chromenes, lapachenole, was photoactivated to a product that irreversibly inhibited CYP3A4 metabolism. Moreover, evidence was provided that lapachenole was a photoaffinity ligand that affected the CYP3A4 active site, since active-site substrate/inhibitors of this enzyme protected it from lapachenole-mediated photoinactivation. Elucidation of structure/function relationships of cytochrome P450s is an important goal in understanding the metabolic fate of many drugs and other chemicals. Identifying sites of substrate recognition and interaction is a critical element in achieving this goal.

In the present work, we determined that the PAL lapachenole is a substrate for CYP3A4, but upon photolysis it largely inactivates CYP3A4 by forming adducts to cysteine residues in two different regions of the CYP3A4 structure. On the basis of enzymatic digestion of the probe-labeled protein and mass spectrometric analyses of the labeled peptides, Cys-98 of the B−B′ loop and Cys-468 at the end of the L-helix are the major sites of adduction. These data provide the first direct evidence that lapachenole, as a substrate, physically interacts with the N-terminal SRS-1 domain of CYP3A4. The results significantly extend previous site-directed mutagenesis and kinetic studies by providing additional physicochemical evidence for the crucial role of

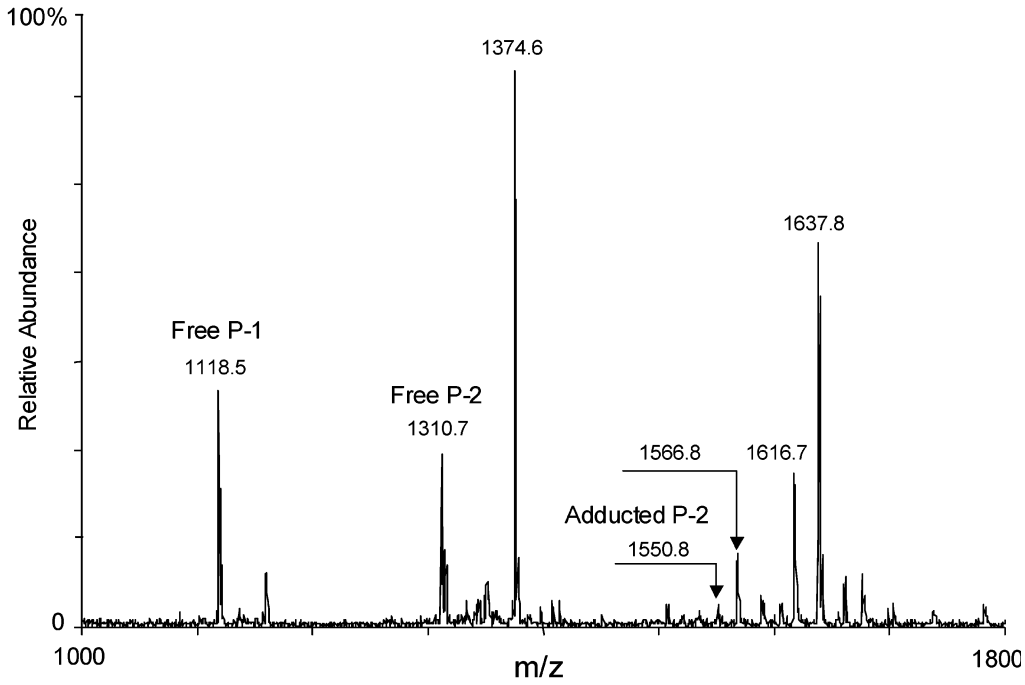

FIGURE 6: MALDI-TOF MS of the collected fluorescent peptide fraction (experiment performed on a Biflex III MALDI-TOF mass spectrometer).

Table 1: Peptides Identified by MALDI-TOF MS from the Fluorescent Fraction

sequence positions	molecular mass (Da)	sequence[a]	modification
97−105	1118.5	ECYSVFTNR	
459−469	1310.7	VLQNFSFKPCK	
97−105	1374.6	E*CYSVFTNR	oxidation
459−469	1550.8	VLQNFSFKP*CK	
459−469	1566.8	VLQNFSFKP*CK	oxidation
497−511	1616.7	DGTVSGASTHHHHHH	
269−282	1637.8	VDFLQLMIDSQNSK	

[a] An asterisk indicates the cysteines are adducted by lapachenole.

this domain for substrate recognition and binding (*26*, *27*, *34*).

Lapachenole is a substrate of CYP3A4 that can be metabolized to three different monooxygenated products (Figures 1 and 2). The exact chemical structures are not fully characterized at this point, but for two of these metabolites, metabolite 2 and 3, the hydroxylation is localized to one of the geminal methyl groups on the chromene ring on the basis of the LC/ESI MS/MS analysis. This result is consistent with the previous finding that the incorporation of photolabel into protein was markedly inhibited in the presence of other CYP3A4 substrates and/or inhibitors (companion paper in this issue). This result also supports the hypothesis that lapachenole binds, as a substrate, within the active site of CYP3A4.

The chemical structure of lapachenole provided a useful fluorescent tag to detect protein and small peptide adducts of CYP3A4 as shown in Figures 3 and 5, respectively. The excitation and emission wavelengths were selected on the basis of the fluorescence spectrum of the lapachenole GSH conjugate. Fluorescence was specifically associated with the apoprotein of CYP3A4 and not with cytochrome b_5, P450 reductase, or CYP3A4 heme as indicated in Figure 3B. This finding agrees with the fact that no other protein adducts, except for those associated with CYP3A4, were detected by LC/MS. Due to their fluorescence, lapachenole-adducted proteins and peptides could conveniently be purified by use of an HPLC system coupled to a fluorescence detector. This was important inasmuch as purification of the adducted peptides dramatically decreased the complexity of the tryptic peptide pool and thereby increased the ability to analyze the peptide adducts by mass spectrometry.

Mass spectrometric analysis of the fluorescent CYP3A4 peak revealed two protein species with average MMs of 57 280 ± 3 and 57 520 ± 3 Da, as shown in Figure 4. On the basis of the peak heights, there is approximately 60% of the CYP3A4 protein covalently labeled by lapachenole (Figure 4). Meanwhile, nearly 80% of enzyme activity was lost when the CYP3A4 protein was labeled by lapachenole under the same conditions (Chart 1 in the companion paper in this issue). This difference could result from a difference in ionization properties between the labeled and unlabeled proteins, since adducted proteins are often less likely to ionize as efficiently as their native proteins. The mass shift of 240 Da showed that only one molecule of lapachenole was bound per molecule of CYP3A4 protein (Figure 4). Monoadduction occurred even when the probe concentration was increased to 1 mM (data not shown). Since loss of CYP3A4 CO binding capacity and extensive enzyme inactivation were previously observed upon photolysis in the presence of lapachenole (companion paper in this issue), it is likely that inactivation results from specific covalent modification of the apoprotein of CYP3A4 by the chromene.

Trypsinolysis of the adducted CYP3A4 yielded a multitude of smaller peptides separated by HPLC and detectable by UV (Figure 5A) but only two major fluorescent peptide adducts, P-1 and P-2 (Figure 5B). MALDI-TOF MS analysis of the collected fluorescent peptide fraction showed the presence of several peptides (Figure 6 and Table 1). Since the peptides labeled free P-1 and free P-2 do not elute in this fraction, they apparently result from breakdown of the

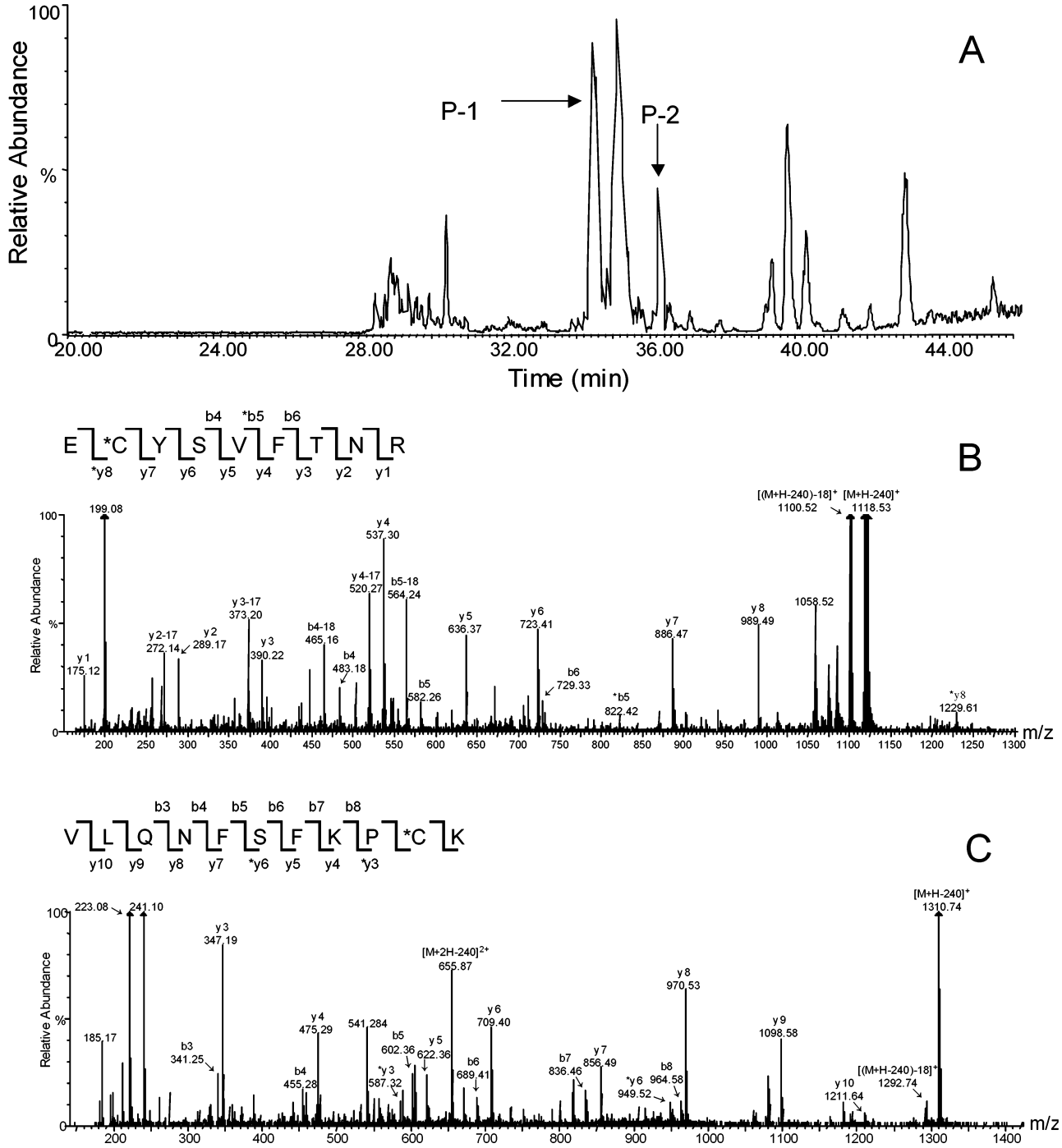

FIGURE 7: (A) Nano-LC/ESI MS base-peak chromatogram of the collected fluorescent fraction. Adducted peptides P-1 and P-2 were eluted at 34.5 and 36.3 min, respectively; Nano-LC/ESI MS/MS spectra of lapachenole-bound CYP3A4 peptide adducts P-1 (B) and P-2 (C) are also shown (experiment performed in an API-US QTOF mass spectrometer).

lapachenole-adducted peptides. An ion at $m/z = 1550.8$ for the P-2 adduct was observed along with an oxidized product at $m/z = 1566.8$, presumably the cysteine sulfoxide. In addition, an ion at $m/z = 1374.6$ corresponds to a similar oxidized product of the lapachenole-adducted P-1. It is assumed that the oxidized products are formed during protein digestion since there is no indication of major amounts of monooxygenated CYP3A4 adducts. Similar behavior was observed under conditions of nano-LC/ESI MS for these compounds even when the cone voltage (responsible for in-source fragmentation) was lowered from 40 to 25 V. Although $[M + H]^+$ ions were observed for adducted peptides P-1 and P-2, ions for other peptides, including free P-1 and P-2, were also present in the ion chromatogram of the nano-LC-separated sample. Since free P-1 and P-2 do not elute in this fraction, they are a result of in-source decomposition. It is noteworthy that the lapachenole GSH conjugate also decomposes under these conditions to generate a base peak ion for protonated GSH and ions at $m/z = 241$ and 199 for protonated lapachenole and its $[M + H - 42]^+$ ion, respectively (companion paper in this issue). Although the decomposition of lapachenole adducts in both MALDI and ESI is undesirable because it limits the sensitivity for detecting these compounds by reducing their signal intensi-

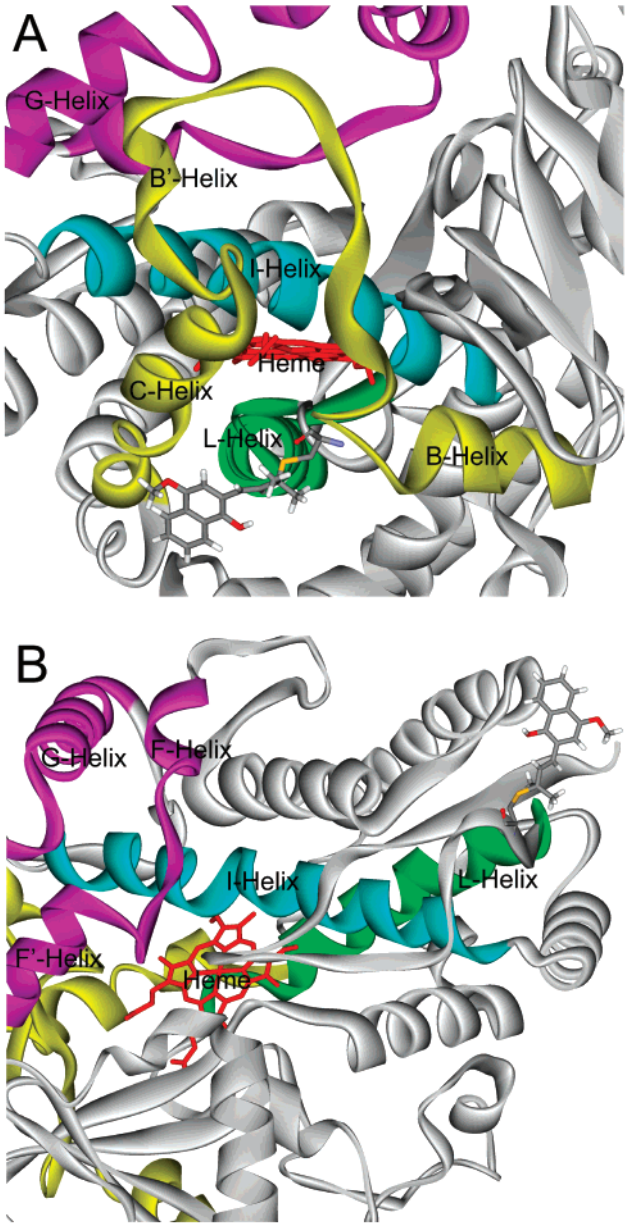

FIGURE 8: Formation of lapachenole Michael adducts in CYP3A4. A partial structure of the complexed CYP3A4 crystal structure is shown with Cys-98 (A) and Cys-468 (B) adducted by lapachenole. The B−C helix loop region (yellow) is shown with the sulfhydryl group of Cys-98 adducted with lapachenole. The I-helix (cyan), L-helix (green), and F/G helix loop (magenta) are also shown with respect to a stick model of the heme (red). The rendering was done in WebLab Viewer Lite 4.0 as described under Experimental Procedures.

ties, such decomposition can be advantageous for locating the adducts in a MALDI spectrum or in an LC MS/MS chromatogram. One can easily identify these adducts by screening the MALDI spectra of enriched adduct fractions for peaks separated by the molecular weight of lapachenole (240.1 Da). This strategy was successful in locating the peptide adduct of P-2 (Figure 6) but failed in the case of the adduct P-1 because no signal was detected for the corresponding protonated peptide adduct. The MS/MS spectra of the two lapachenole adducts shown in Figure 7 have very strong signals either at $m/z = 199.1$ (Figure 7B) or at $m/z = 241.1$ (Figure 7C), which are the ions associated with lapachenole as already discussed. The location of lapachenole in adduct P-1 is on the cysteine residue as determined by the mass difference of 240 Da between the expected y8 and *y8 ions. Although the location of lapachenole in adduct P-2 is less certain, it is most likely on the cysteine residue rather than proline or lysine since the lapachenole photolysis product is a conjugated "soft" electrophilic dienone that would more efficiently react with a "soft" nucleophile, such as a cysteine thiol group.

Thus, two cysteine residues, Cys-98 and Cys-468, were identified as the modification sites of lapachenole in the photolabeled CYP3A4. From the crystal structure, Cys-98 is located within the putative flexible B−B′ loop region in close proximity to the proposed SRS-1 region of CYP3A4, while Cys-468 is located in the end of the L-helix near the SRS-6 region of the protein (Figure 8). Important insights have resulted from the cocrystallization of CYP3A4 and its inhibitor/substrates metyrapone or progesterone (*26*). The ligand-free and complexed structures diverge at residue Val95 toward the end of helix B, at the beginning of the B−B′ loop region, but converge again at residue Phe102. Peptide adduct P-1 (positions 97−105) identified in this study overlaps considerably with this flexible loop region. In the active-site cavity of CYP3A4, the solvent-accessible molecular surface branches distal to the heme, to form two channels separated by the B−C loop and the B′ helix. Moreover, the crystal data suggest that small movements of the B−C loop could facilitate substrate entry into the active site and increase the active-site volume (*26*). Other studies have concluded that the effect of several mutations in the SRS-1 region has a profound impact on catalysis and/or substrate specificity. Roussel et al. (*34*) reported that the highly conserved residue S119 in the SRS-1 region is a key determinant of CYP3A4 specificity and likely to be involved in substrate binding and/or substrate recognition. In other crystallized P450s, this region contains the active-site residues V113 and F114 of CYP2C9 (*35*), F87 and T88 of P450BM-3 (*36*), T101 of P450cam (*37*), G91of P450eryF (*38*), T103 of P450terp (*39*), and S75 of P450nor (*40*), all of which have been shown to be involved in substrate interactions. While SRS-1 is one of the most variable regions among P450s of known crystal structure, with very different lengths and orientations as well as very low sequence identity (*41*), alignment studies have shown that Cys-98 is highly conserved in all CYP3A family members (*16*). In this respect, our data provide the first direct evidence that lapachenole, as a substrate, physically interacts with the N-terminal SRS-1 region of CYP3A4. These results significantly extend previous site-directed mutagenesis and kinetic studies by providing additional physicochemical evidence for the crucial role of this region in its catalytic activity.

Although lapachenole modification of another cysteine residue, Cys-468, also decreases CYP3A4 activity, visual inspection of the complexed crystal structure (Figure 8B) suggests that Cys-468 is located more on the outer surface of the enzyme. However, Cys-468 is positioned near the SRS-6 region at the end of the L-helix of CYP3A4, on which the cysteinal heme ligand, Cys-442, is located. A multiple sequence alignment study shows that Cys-468 is highly conserved in all CYP3A family members (*16*). A recent study has also shown that Gly-480 in the SRS-6 domain of CYP3A4 is directly involved in progesterone 6β- and 21-dihydroxylation (*42*). Interestingly, on the basis of a crystal structure of CYP3A4 (*26*), progesterone binds in a position

distant from the active site. Lapachenole also appears to bind at a site removed from the active site on the basis of the photoinactivation studies presented in this paper. The significance of this apparent second binding site is not clear at the present time.

The conversion of the P450 spectrum to a P420 spectrum usually indicates that a conformational change in the heme environment results in the inability of CO to bind to the active-site heme. As previously observed (*43*), modest changes in protein structure are all that is required to effect a change from P450 to P420. As indicated by the lapachenole-adducted CYP3A4 structure, the Cys-98 lapachenole adduct is located in close proximity (~7 Å) to the CYP3A4 heme group on the B−B′ helix that forms part of the substrate access channel. The adduct likely restricts access of substrates to the active site and induces subtle conformational changes that affect the heme environment leading to the P420 spectrum. Cys-468, the other site of adduction, is at the end of the L-helix on which the cysteinyl group that ligands to the heme iron, Cys-442, is located. Thus, it is not unreasonable to conclude that binding of lapachenole at Cys-468 causes enough of a conformational change to affect the Cys-442 heme iron binding.

In conclusion, we have developed a novel type of fluorescent PAL to probe mammalian cytochrome P450 structures and characterized modifications of CYP3A4 by photoaffinity labeling with one of these chromenes, lapachenole. MALDI-TOF MS and LC/ESI MS/MS were used to identify two distinct peptides that were modified by lapachenole, one at Cys-98 and the other most probably at Cys-468. Since both residues are located within relatively flexible loop regions that have previously been shown to affect substrate recognition and catalysis, these adducts may inhibit CYP3A4 enzyme activity by inhibiting substrate binding to the active site directly or by blocking an access channel, or by other conformational effects that perturb redox partner interactions. Additional studies are underway with site-directed mutants to investigate these possible mechanisms.

ACKNOWLEDGMENT

E. coli DH5α containing the expression vector pCW 3A4-His6 and human cytochrome b_5 expression plasmid were kindly provided by Dr. Ron Estabrook, University of Texas Southwest Medical Center, Dallas, TX. We thank Dr. Mike Dabrowski for technical assistance.

SUPPORTING INFORMATION AVAILABLE

Deconvoluted spectra of P450 reductase and cytochrome b_5 and ESI mass spectrum of the heme of CYP3A4 from LC/ESI MS analysis of the reconstituted CYP3A4 system treated with lapachenole under photolytic conditions (PDF). This material is available free of charge via the Internet at http://pubs.acs.org.

REFERENCES

1. Guengerich, F. P. (1995) in *Cytochrome P450: structure, mechanism, and biochemistry* (Ortiz de Montellano, P. R., Ed.) pp 473−536, Plenum Press, New York.
2. Fuhr, U., Weiss, M., Kroemer, H. K., Neugebauer, G., Rameis, H., Weber, W., and Woodcock, B. G. (1996) Systematic screening for pharmacokinetic interactions during drug development, *Int. J. Clin. Pharmacol. Ther. 34*, 139−151.
3. Williams, P. A., Cosme, J., Ward, A., Angove, H. C., Matak, Vinkovic, D., and Jhoti, H. (2003) Crystal structure of human cytochrome P450 2C9 with bound warfarin, *Nature 424*, 464−468.
4. Wester, M. R., Johnson, E. F., Marques-Soares, C., Dijols, S., Dansette, P. M., Mansuy, D., and Stout, C. D. (2003) Structure of mammalian cytochrome P450 2C5 complexed with diclofenac at 2.1 Å resolution: evidence for an induced fit model of substrate binding, *Biochemistry 42*, 9335−9345.
5. Davydov, R., Kofman, V., Fujii, H., Yoshida, T., Ikeda-Saito, M., and Hoffman, B. M. (2002) Catalytic mechanism of heme oxygenase through EPR and ENDOR of cryoreduced oxy-heme oxygenase and its Asp 140 mutants, *J. Am. Chem. Soc. 124*, 1798−1808.
6. Dabrowski, M. J., Schrag, M. L., Wienkers, L. C., and Atkins, W. M. (2002) Pyrene−pyrene complexes at the active site of cytochrome P450 3A4: evidence for a multiple substrate binding site, *J. Am. Chem. Soc. 124*, 11866−11867.
7. He, Y. A., He, Y. Q., Szklarz, G. D., and Halpert, J. R. (1997) Identification of three key residues in substrate recognition site 5 of human cytochrome P450 3A4 by cassette and site-directed mutagenesis, *Biochemistry 36*, 8831−8839.
8. Harlow, G. R., and Halpert, J. R. (1998) Analysis of human cytochrome P450 3A4 cooperativity: construction and characterization of a site-directed mutant that displays hyperbolic steroid hydroxylation kinetics, *Proc. Natl. Acad. Sci. U.S.A. 95*, 6636−6641.
9. Khan, K. K., He, Y. Q., Domanski, T. L., and Halpert, J. R. (2002) Midazolam oxidation by cytochrome P450 3A4 and active-site mutants: an evaluation of multiple binding sites and of the metabolic pathway that leads to enzyme inactivation, *Mol. Pharmacol. 61*, 495−506.
10. Lightning, L. K., Jones, J. P., Friedberg, T., Pritchard, M. P., Shou, M., Rushmore, T. H., and Trager, W. F. (2000) Mechanism-based inactivation of cytochrome P450 3A4 by L-754,394, *Biochemistry 39*, 4276−4287.
11. Regal, K. A., Schrag, M. L., Kent, U. M., Wienkers, L. C., and Hollenberg, P. F. (2000) Mechanism-based inactivation of cytochrome P450 2B1 by 7-ethynylcoumarin: verification of apo-P450 adduction by electrospray ion trap mass spectrometry, *Chem. Res. Toxicol. 13*, 262−270.
12. Darbandi-Tonkabon, R., Hastings, W. R., Zeng, C. M., Akk, G., Manion, B. D., Bracamontes, J. R., Steinbach, J. H., Mennerick, S. J., Covey, D. F., and Evers, A. S. (2003) Photoaffinity labeling with a neuroactive steroid analogue. 6-azi-pregnanolone labels voltage-dependent anion channel-1 in rat brain, *J. Biol. Chem. 278*, 13196−13206.
13. Kon, N., and Suhadolnik, R. J. (1996) Identification of the ATP binding domain of recombinant human 40-kDa 2′,5′-oligoadenylate synthetase by photoaffinity labeling with 8-azido-[α-^{32}P]ATP, *J. Biol. Chem. 271*, 19983−19990.
14. Hasemann, C. A., Kurumbail, R. G., Boddupalli, S. S., Peterson, J. A., and Deisenhofer, J. (1995) Structure and function of cytochromes P450: a comparative analysis of three crystal structures, *Structure 3*, 41−62.
15. Szklarz, G. D., and Halpert, J. R. (1997) Molecular modeling of cytochrome P450 3A4, *J. Computer-Aided Mol. Design. 11*, 265−272.
16. Lewis, D. F. V., Eddershaw, P. J., Goldfarb, P. S., and Tarbit, M. H. (1996) Molecular modelling of CYP3A4 from an alignment with CYP102: identification of key interactions between putative active site residues and CYP3A-specific chemicals, *Xenobiotica 26*, 1067−1086.
17. Locuson, C. W., 2nd, Rock, D. A., and Jones, J. P. (2004) Quantitative binding models for CYP2C9 based on benzbromarone analogues. *Biochemistry 43*, 6948−6958.
18. Afzelius, L., Zamora, I., Ridderstrom, M., Andersson, T. B., Karlen, A., and Masimirembwa, C. M. (2001) Competitive CYP2C9 inhibitors: enzyme inhibition studies, protein homology modeling, and three-dimensional quantitative structure−activity relationship analysis. *Mol. Pharmacol. 59*, 909−919.
19. Gartner, C. A. (2003) Photoaffinity ligands in the study of cytochrome p450 active site structure, *Curr. Med. Chem. 10*, 671−689.
20. Yun, C. H., Hammons, G. J., Jones, G., Martin, M. V., Hopkins, N. E., Alworth, W. L., and Guengerich, F. P. (1992) Modification of cytochrome P450 1A2 enzymes by the mechanism-based inactivator 2-ethynylnaphthalene and the photoaffinity label 4-azidobiphenyl, *Biochemistry 31*, 10556−10563.

21. Miller, J. P., and White, R. E. (1994) Photoaffinity labeling of cytochrome P450 2B4: capture of active site heme ligands by a photocarbene, *Biochemistry 33*, 807−817.
22. Antonovic, L., Hodek, P., Smrcek, S., Novak, P., Sulc, M., and Strobel, H. W. (1999) Heterobifunctional photoaffinity probes for cytochrome P450 2B, *Arch. Biochem. Biophys. 370*, 208−215.
23. Cvrk, T., and Strobel, H. W. (1998) Photoaffinity labeling of cytochrome P4501A1 with azidocumene: identification of cumene hydroperoxide binding region, *Arch. Biochem. Biophys. 349*, 95−104.
24. Cvrk, T., Hodek, P., and Strobel, H. W. (1996) Identification and characterization of cytochrome P4501A1 amino acid residues interacting with a radiolabeled photoaffinity diazido-benzphetamine analogue, *Arch. Biochem. Biophys. 330*, 142−152.
25. Becker, R. S., and Michl, J. (1966) Photochromism of synthetic and naturally occurring 2*H*-chromenes and 2*H*-pyrans, *J. Am. Chem. Soc. 88*, 5931−5933.
26. Williams, P. A., Cosme, J., Vinkovi_, D. M., Ward, A., Angove, H. C., Day, P. J., Vonrhein, C., Tickle, I. J., and Jhoti, H. (2004) Crystal Structures of Human Cytochrome P450 3A4 Bound to Metyrapone and Progesterone, *Science 305*, 683−686.
27. Yano, J. K., Wester, M. R., Schoch, G. A., Griffin, K. J., Stout, C. D., and Johnson, E. F. (2004) The structure of human microsomal cytochrome P450 3A4 determined by X-ray crystallography to 2.05 Å resolution, *J. Biol. Chem. 279*, 38091−38094.
28. Gillam, E. M., Baba, T., Kim, B. R., Ohmori, S., and Guengerich, F. P. (1993) Expression of modified human cytochrome P450 3A4 in *Escherichia coli* and purification and reconstitution of the enzyme, *Arch. Biochem. Biophys. 305*, 123−31.
29. Holmans, P. L., Shet, M. S., Martin-Wixtrom, C. A., Fisher, C. W., and Estabrook, R. W. (1994) The high-level expression in *Escherichia coli* of the membrane-bound form of human and rat cytochrome b_5 and studies on their mechanism of function, *Arch. Biochem. Biophys. 312*, 554−565.
30. Chen, W., Koenigs, L. L., Thompson, S. J., Peter, R. M., Rettie, A. E., Trager, W. F., and Nelson, S. D. (1998) Oxidation of acetaminophen to its toxic quinone imine and nontoxic catechol metabolites by baculovirus-expressed and purified human cytochromes P450 2E1 and 2A6, *Chem. Res. Toxicol. 11*, 295−301.
31. Kennedy, R. T., and Jorgenson, J. W. (1989) Preparation and evaluation of packed capillary liquid chromatography columns with inner diameters from 20 to 50 micrometers, *Anal. Chem. 61*, 1128−1135.
32. Shaw, P. M., Hosea, N. A., Thompson, D. V., Lenius, J. M., and Guengerich, F. P. (1997) Reconstitution premixes for assays using purified recombinant human cytochrome P450, NADPH-cytochrome P450 reductase, and cytochrome b_5, *Arch. Biochem. Biophys. 348*, 107−115.
33. Guex, N., and Peitsch, M. C. (1997) SWISS-MODEL and the Swiss-PdbViewer: an environment for comparative protein modeling, *Electrophoresis 18*, 2714−2723.
34. Roussel, F., Khan, K. K., and Halpert, J. R. (2000) The importance of SRS-1 residues in catalytic specificity of human cytochrome P450 3A4, *Arch. Biochem. Biophys. 374*, 269−278.
35. Haining, R. L., Jones, J. P., Henne, K. R., Fisher, M. B., Koop, D. R., Trager, W. F., and Rettie, A. E. (1999) Enzymatic determinants of the substrate specificity of CYP2C9: role of B′−C loop residues in providing the π-stacking anchor site for warfarin binding, *Biochemistry 38*, 3285−3292.
36. Ravichandran, K. G., Boddupalli, S. S., Hasemann, C. A., Peterson, J. A., and Deisenhofer, J. (1993) Crystal structure of hemoprotein domain of P450BM-3, a prototype for microsomal P450's, *Science 261*, 731−736.
37. Poulos, T. L., Finzel, B. C., Gunsalus, I. C., Wagner, G. C., and Kraut, J. (1985) The 2.6-A crystal structure of *Pseudomonas putida* cytochrome P-450, *J. Biol. Chem. 260*, 16122−16130.
38. Cupp-Vickery, J. R., and Poulos, T. L. (1995) Structure of cytochrome P450eryF involved in erythromycin biosynthesis, *Nat. Struct. Biol. 2*, 144−153.
39. Hasemann, C. A., Ravichandran, K. G., Peterson, J. A., and Deisenhofer, J. (1994) Crystal structure and refinement of cytochrome P450terp at 2.3 A resolution, *J. Mol. Biol. 236*, 1169−1185.
40. Zhang, L., Kudo, T., Takaya, N., and Shoun, H. (2002) The B′ helix determines cytochrome P450nor specificity for the electron donors NADH and NADPH, *J. Biol. Chem. 277*, 33842−33847.
41. Johnson, E. F. (2003) The 2002 Bernard B. Brodie Award lecture: deciphering substrate recognition by drug-metabolizing cytochromes P450, *Drug Metab. Dispos. 31*, 1532−1540.
42. Xue, L., Zgoda, V. G., Arison, B., and Correia, M. A. (2003) Structure−function relationships of rat liver CYP3A9 to its human liver orthologs: site-directed active site mutagenesis to a progesterone dihydroxylase, *Arch. Biochem. Biophys. 409*, 113−126.
43. Martinis, S. A., Blanke, S. R., Hager, L. P., Sligar, S. G., Hui Bon Hoa, G., Rux, J. J., and Dawson, J. H. (1996) Probing the heme iron coordination structure of pressure-induced cytochrome $P420_{cam}$, *Biochemistry 35*, 14530−14536.

BI048228C